Adaptive Edge Masking Based on TV Decomposition and Adjacent Similarity for Digital Watermarking

Jianwei Guo[1], Yana Zhang [1], Shuang Zhi [1], Pamela Cosman[2]

[1]*Communication University of China, Beijing, China*
[2]*Department of Electrical and Computer Engineering, University of California, San Diego, USA*

Abstract—**Digital watermarking algorithms usually focus on texture masking due to the increasing noise insensitivity in texture regions. However, not all images have abundant texture regions. For images containing primarily edges and smooth regions, an image watermark should be embedded in edge areas. An adaptive edge-masking based on Total Variation (TV) decomposition for digital watermarking is proposed in this paper. First, edge detection based on the TV decomposition is applied to get accurate edges. After that, edge masking tends to be effective when the hidden signal has a similar direction and frequency as edges in the adjacent area. At last, the embedding intensity and position are determined adaptive to the image content. Experimental results show that our algorithm has good imperceptibility and is more robust than the algorithm without edge masking.**

Keywords—edge masking; JND; digital watermarking

I. INTRODUCTION

Effective copyright protection for digital media is an urgent problem, and digital watermarking is one of the best methods to protect digital content. It is a technique to embed copyright information into digital content such as videos and images. The most important factors to consider in digital image watermarking are imperceptibility and robustness. That is, the watermark needs to be invisible and resistant to tampering.

In early watermarking techniques, image content was overlooked. In Cox's [1] proposal, a sequence of watermark bits was embedded into n highest DCT coefficients in the entire image. For balancing imperceptibility and robustness of watermarking, many digital watermarking schemes based on the human visual system (HVS) burst onto the scene. Humans are insensitive to additive noise in areas of high frequency or high brightness. Kankanhalli [2] allowed every pixel to have its JND (Just Noticeable Distortion) values for the mask based on image luminance. In [3], Barni's JND model in the DWT domain included frequency sensitivity, luminance masking, and contrast masking, three important masking effects in the HVS. But these JND models take signal characteristics (frequency, luminance and contrast) into account, rather than image content characteristics (edges, texture, corners and objects).

In [4], a JND model was proposed containing the features of texture, corners, edges and luminance. Texture masking is the main trend among digital watermarking algorithms at present, and several schemes are reported in the literature. In [5], a DFT based 3×3 sub-image scheme introduced the watermark into the highly textured regions of sub-images. Wu [6] proposed a model which combined luminance adaptation and texture masking with a nonlinear formula. Li [7] described an improved perceptual mask using an arrangement of SIFT (scale invariant feature points). The mask has low JND values in both edge and flat areas, and high values only in highly textured regions. Concentrating on texture regions, in [8] a digital watermarking algorithm based on texture blocks and edge detection in the DWT domain was proposed. The watermark was embedded into the high frequency and low frequency sub-bands in texture blocks. In these watermarking schemes based on the HVS, as the watermark was embedded in textured regions, edge detection was mainly used for separating texture from non-texture in the original image. Edge masking was not actually considered in those JND models. Also, those algorithms are not fit for images with few texture characteristics. For example, images with tiles, railings, and buildings might not have enough capacity in the texture regions for information hiding.

It has been shown in visual psychological experiments [9, 10] that the masking effect is strongest when the signal being masked has the same direction and frequency as the background. Also, the masking threshold value in the adjacent area of the edge is 3 or 4 times larger than that in the far-field area. Accordingly, we assume that edge masking would be most efficient when the signal to be hidden has a similar direction and frequency as the edge in the adjacent area. Inspired by this adjacent similarity concept, we propose a digital watermarking algorithm in the DWT domain based on adaptive edge masking. Edge information is separated from non-edge information in the original image through structure extraction from texture via relative total variation [11] and then directional edges (vertical, horizontal, diagonal) are extracted individually for modeling edge masking. Finally, the embedding intensity and position are determined adaptively to the image content.

II. EDGE MASKING BASED ON ADJACENT SIMILARITY

A. Edge Detection Using Total Variation

For modeling edge masking, we have to separate edge and texture regions precisely. Often, image edges are mixed with textured regions. False edges may come from noise and texture. We use Total Variation (TV) to segment the original

978-1-4673-9088-0/15/$31.00 ©2015 IEEE

image into a structure image (smooth with sharp edges) and a texture image. This model effectively separates edges and texture. In our work, we use a recent algorithm [11] to get the structural image. In [11], Xu used a model from [12], expressed as:

$$\arg\min_{S}\sum_{p}(S_p - I_p)^2 + \lambda\cdot\left(\frac{D_x(p)}{L_x(p)+\varepsilon}+\frac{D_y(p)}{L_y(p)+\varepsilon}\right) \quad (1)$$

$$D_x(p)=\sum_{q\in R(p)} g_{p,q}\cdot\left|(\partial_x S)_q\right| \quad (2)$$

$$D_y(p)=\sum_{q\in R(p)} g_{p,q}\cdot\left|(\partial_y S)_q\right| \quad (3)$$

$$L_x(p)=\left|\sum_{q\in R(p)} g_{p,q}\cdot(\partial_x S)_q\right| \quad (4)$$

$$L_y(p)=\left|\sum_{q\in R(p)} g_{p,q}\cdot(\partial_y S)_q\right| \quad (5)$$

where I is the input image's luminance and p indexes 2D pixels. S is the resulting structure image. The first term $(S_p - I_p)^2$ tries to make the resulting structure image similar to the input image. The second term tries to flatten neighboring image pixel values, removing the texture. λ ranges from 0.01~0.03 [11]. The variable q indexes all pixels in the rectangular region centered at pixel p and $g_{p,q}$ is the Gaussian kernel function:

$$g_{p,q}\propto\exp\left(-\frac{(x_p-x_q)^2+(y_p-y_q)^2}{2\sigma^2}\right) \quad (6)$$

Comparison images based on TV [11] are shown in Fig. 1.

(a) (b)

Fig. 1. (a) Original image (b) Structural image by TV

Then, we use a Canny edge detector to obtain edges from the structure image. We compared the accuracy of edge extraction using Canny edge detectors with thresholds of 0.5 and 0.1 as well as TV combined with Canny edge detection with a threshold of 0.1. Results show that the edge maps detected by the Canny detector alone contain a few texture details (Fig. 2.1.c). As we increase the threshold of the Canny edge detector, edges can be extracted quite precisely from highly textured images (Fig. 2.1.d). But images with less texture would miss some edges with the same threshold (Fig. 2.2.d). The experiment shows that TV combined with Canny edge detection (Figs. 2.1.b and 2.2.b) separates texture and edges more precisely and is adaptive to images with different kinds of content.

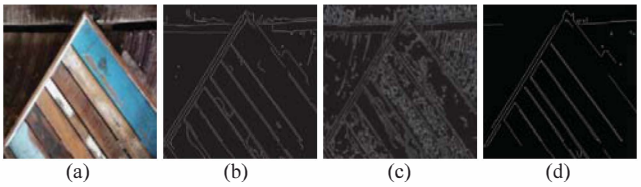

(a) (b) (c) (d)

Fig. 2.1 woods

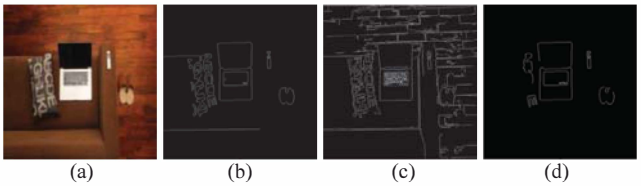

(a) (b) (c) (d)

Fig. 2.2 sofa

Fig. 2. Comparison of different edge detection methods. (a) Original image (b) TV combined with Canny edge detector (threshold=0.1) (c) Canny edge detector (threshold=0.1) (d) Canny edge detector(threshold=0.5)

B. Edge Masking

An important characteristic of edges is that additive noise is less discernible when it is hidden in the same direction and frequency as background edges. We call this "adjacent similarity." If a watermark is embedded into the vertical sub-band, the edges in the watermarked image (shown as Fig. 3.b) are much smoother than those in Fig. 3.a, which is watermarked in the horizontal sub-band. This is because the background edges of the original image are mostly vertical. The watermark is more imperceptible, benefitting from edge masking based on adjacent similarity.

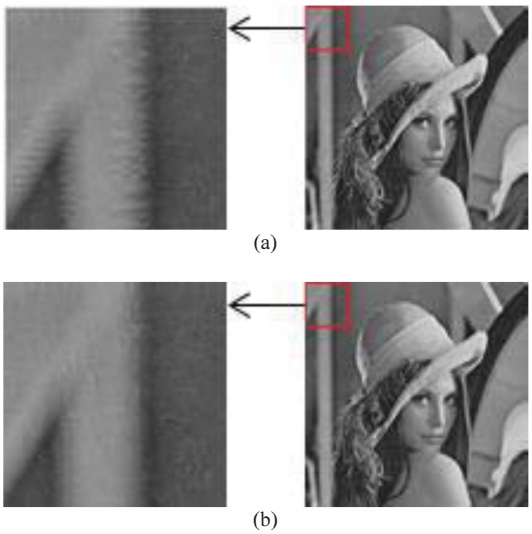

(a)

(b)

Fig. 3. (a) Watermarked images without adjacent similarity (b) Watermarked image with adjacent similarity

We consider three main edge directions: horizontal, vertical, and diagonal. First, the edge image undergoes a 3-level Haar DWT decomposition. We take frequency sensitivity $Frq(l,\theta)$ and luminance masking $Lum(l,i,j)$ into account, which are referenced from [3]. The preliminary $JND_{preli}(i,j,\theta,l)$ (Fig. 4b) of the edge image depends on the orientation angle θ, resolution level l, and location (i,j) and is given by the followed functions (7) – (9), where α=0.5 [3].

$$JND_{preli}(i,j,\theta,l) = \alpha \cdot Frq(l,\theta) \cdot Lum(l,i,j) \tag{7}$$

$$Frq(l,\theta) = \begin{Bmatrix} 1.5 & if\ \theta = HH \\ 1.2 & if\ \theta = HL\ or\ LH \\ 1 & if\ \theta = LL \end{Bmatrix} \cdot \begin{Bmatrix} 1.00 & if\ l = 1 \\ 0.32 & if\ l = 2 \\ 0.16 & if\ l = 3 \end{Bmatrix} \tag{8}$$

$$Lum(l,i,j) = 1 + \frac{1}{256} I_l^{LL}(l,i,j) \tag{9}$$

We apply a Canny edge detector (with the threshold of 0.4) and Gaussian filter into the preliminary JND image to obtain $JND_{proce}(i,j)$. Next, the $JND_{overall}(i,j)$ (Fig. 4c) is expressed as:

$$JND_{overall}(i,j) = JND_{preli}(i,j) + \alpha \cdot JND_{proce}(i,j) - \beta \cdot \left\{ \min\left(JND(i,j), JND_{proce}(i,j) \right) \right\} \tag{10}$$

To further improve edge accuracy, we evaluate the weight α in range between 0 and 0.1 with the step size of 0.01 and the weight β in range between 0 and 1 with the step size of 0.1 on multiple images. In this paper, we obtain more accurate edge when the weight α is 0.02 and the weight β is 0.3.

Then, three directionally detailed sub-bands are filtered to get the gradient in the horizontal and vertical directions. We use the arctan function to obtain the angles ($Thta_h(i,j)$, $Thta_v(i,j)$), $Thta_d(i,j)$) of different directional edges in different sub-bands. The angle range from 0° to 15° corresponds to pixels on horizontal edges, 75° to 90° are on vertical edges, and the others are diagonal. Finally, different JND values in each direction are denoted:

$$JND_{ori}(i,j) = Thta_{ori}(i,j) \times JND_{overall}(i,j) \quad ori = h,v,d. \tag{11}$$

$JND_h(i,j)$, $JND_v(i,j)$ and $JND_d(i,j)$ denote the JND value for the horizontally, vertically and diagonally detailed sub-bands (HL, LH, HH), shown in Fig. 4d, e, f.

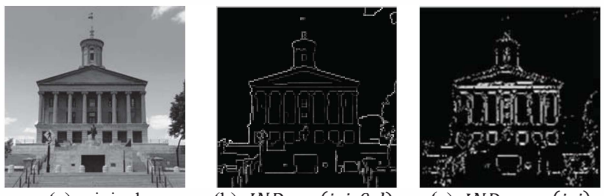

(a) original (b) $JND_{preli}(i,j,\theta,l)$ (c) $JND_{overall}(i,j)$

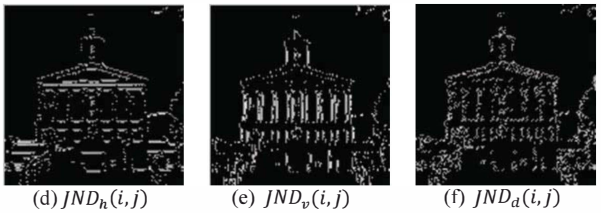

(d) $JND_h(i,j)$ (e) $JND_v(i,j)$ (f) $JND_d(i,j)$

Fig. 4. Original image and JND value maps

III. WATERMARKING ALGORITHM

Inevitably, there are intersectional pixels, where an edge in one direction intersects an edge in another direction. This raises questions on how to embed the watermarking at these locations: which direction these intersections belong to, the order of directional sub-bands being embedded, and the number of watermark bits embedded in each direction. For adapting to different kinds of images, our strategy is proposed below.

The determination of embedding position is related to the ratio of different directional pixels among the whole edge image, expressed as $\frac{Num_{ori}}{Num_{all}}$ (ori = h, v, d). The sub-band with the highest ratio is embedded first, and the number of watermarking bits embedded in different sub-bands is calculated by:

$$N_{ori} = round(ratio_{ori} \cdot N) \tag{12}$$

Intersectional pixels should not be selected repeatedly as different sub-bands are considered. After ruling out the pixels selected for embedding in the first sub-band, we determine the embedding order of the remaining two sub-bands with the same strategy. The embedding positions for different directional sub-bands are shown in Fig. 5.

(a) $JND_h(i,j)$ (b) $JND_v(i,j)$ (c) $JND_d(i,j)$

Fig. 5. Embedding positions in different directional sub-bands

The watermarking embedding algorithm includes the following steps (shown in Fig. 6).

(1) Generate the watermarking sequence through binarization and chaotic scrambling of a copyright image.

(2) Extract the edge information of the original image through TV decomposition and Canny edge detection.

(3) Build the edge masking model described in section II and get each directional JND value: $JND_h(i,j)$, $JND_v(i,j)$ and $JND_d(i,j)$.

(4) Determine the embedding position and embedding strength using:

$$S_{ori}(i,j) = \alpha \cdot JND_{ori}(i,j) \quad ori = h,v,d. \tag{13}$$

(5) Transform the original image into the DWT domain based on a 3-level haar DWT decomposition. The embedding function is represented as:

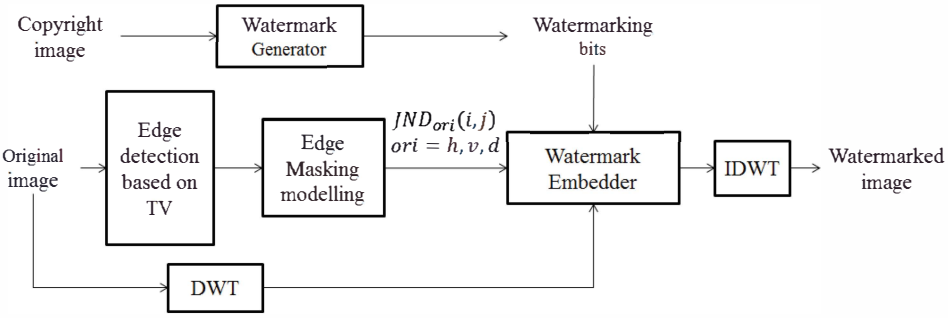

Fig. 6. Watermarking embedding procedure

$$coef'_{ori}(i,j) = \begin{cases} coef_{ori}(i,j) - \mathrm{mod}\left(coef_{ori}(i,j), S_{ori}(i,j)\right) + \frac{S_{ori}(i,j)}{4} & if\ W=0 \,\&\, P=1 \\ coef_{ori}(i,j) - \mathrm{mod}\left(coef_{ori}(i,j), S_{ori}(i,j)\right) + \frac{3\times S_{ori}(i,j)}{4} & if\ W=1 \,\&\, P=1 \\ coef_{ori}(i,j) & if\ P=0 \end{cases} \quad ori = h,v,d \tag{14}$$

(6) After IDWT, get the final watermarked image.

In watermarking detector, if remainder $R(i,j)$ is in $(0,\frac{S(i,j)}{2}]$, the embedded watermark is 0. Or if the remainder is in $(\frac{S(i,j)}{2}, S(i,j)]$, the embedded watermark is 1, expressed as:

$$R(i,j) = \mathrm{mod}\left(coef(i,j), S(i,j)\right) \tag{15}$$

$$W = \begin{cases} 0 & if\ 0 < R(i,j) \le \frac{S(i,j)}{2} \\ 1 & if\ \frac{S(i,j)}{2} < R(i,j) \le S(i,j) \end{cases} \tag{16}$$

After anti-scrambling and undoing the sorting operation, the watermark is obtained.

IV. Experiments and Results

We conduct a comparison between our scheme described in Sec.III (EMAS for short) and a usual watermarking scheme only based on TV decomposition [11] (discarding adjacent similarity and embedding the watermark globally, TVDG for short). We keep the same conditions for them. For the both, the watermark is embedded into HL2, LH2, HH2 (all the directional sub-bands).

Original images with different edge characteristics are all bmp format, size 512×512. The copyright image is shown in size 64×32.

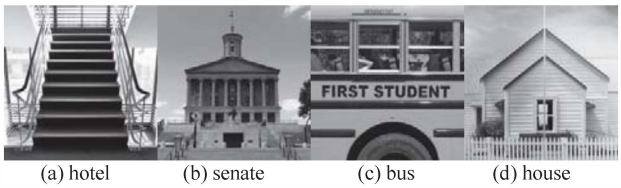

(a) hotel (b) senate (c) bus (d) house

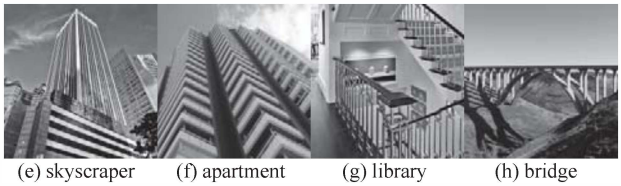

(e) skyscraper (f) apartment (g) library (h) bridge

(i) Copyright image

Fig. 7. Original and copyright images

A. Imperceptibility Assessment

As shown in Fig. 8, watermarks in both pairs of watermarked images are invisible. And the SSIM (Structural Similarity Index Measurement) values of 0.99 are the same for these two images (shown in Table I). The watermarked images are good as the original images.

(a) (b) (c)

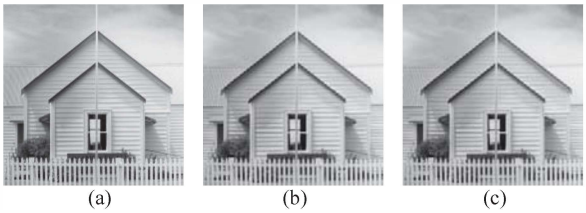

(a) (b) (c)

Fig. 8. (a) Original image (b) The usual sheme (c) Our scheme

TABLE I
PSNR AND SSIM RESULTS IN IMPERCEPTIBILITY ASSESSMENT

Image	SSIM Value		PSNR Value	
	EMAS	TVDG	EMAS	TVDG
Hotel	0.999	0.999	44.14	47.39
Senate	0.998	0.999	46.60	50.31
Bus	0.999	0.999	45.20	48.47
House	0.999	0.999	45.59	48.52
Skyscraper	0.999	0.999	46.07	48.72
Apartment	0.998	0.999	46.22	49.37
Library	0.998	0.999	44.56	47.76
Bridge	0.998	0.999	46.59	49.92

When we turn to PSNR (Peak Signal to Noise Ratio) results, EMAS has a lower PSNR value than that of TVDG. This is because the embedding strength of EMAS has been increased compared to the embedding strength of TVDG while they are both invisible. This can be done because EMAS is based on an edge masking property of the human visual system, which is not captured well by PSNR. The net effect is that EMAS is more robust to attack, as will be shown in the next section.

B. Robustness Assessment

BER (Bit Error Rate) under different attacks with different intensity of attack is taken to assess the robustness of watermarking algorithms. The Stirmark 4.0 is used for creating different attacks for the watermarked images. Attacking type, intensity and BER results are shown in Table II. And EMAS performs well against additive noise, cropping and rotation with specified parameters. The BER for JPEG compression is larger than the BER in other attacks, because we choose all HL, LH and HH sub-bands for embedding and the HH sub-band especially may be heavily compressed in JPEG.

TABLE II
BER RESULTS OF DIFFERENT ATTACKS IN SPECIFIED PARAMETERS

Attack Type	Image Type		
	House	senate	bridge
Additive Noise 0.2dB	0.000	0.000	0.000
JPEG Compression (Q_60)	0.199	0.179	0.298
Cropping 95%	0.034	0.013	0.025
Rotation 0.01	0.001	0.002	0.008

We compared EMAS with TVDG in terms of robustness. In Fig. 9.a, BER results of EMAS in additive noise attacks with intensity from 0.5 to 2.3 dB are all lower than those of TVDG. Especially, the greatest BER difference appeared when the noise intensity is 1.3. And in Fig. 9.c, all tested images perform better than TVDG against additive noise with intensity of 1.1 dB. EMAS shows greater robustness to the attack of additive noise. In Fig. 9.b, BER results for EMAS are all significantly better for quality factors ranging from 10 to 90. Also in Fig. 9.d the BER results for EMAS for all tested images are better than those for TVDG to different degree. EMAS is more robust against JPEG compression compared to TVDG.

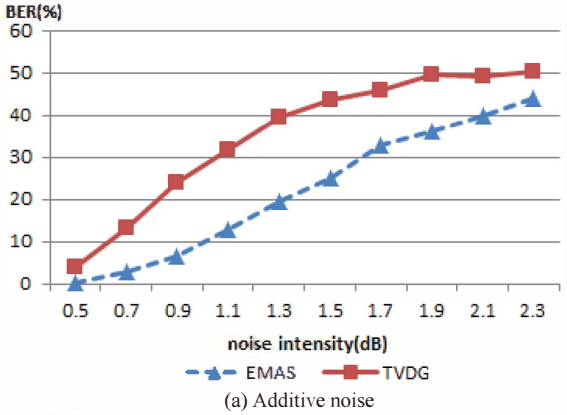

(a) Additive noise

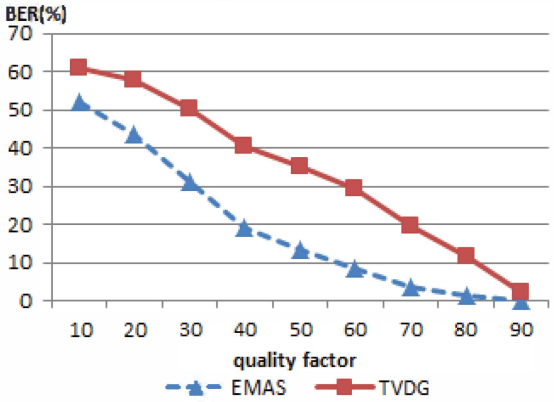

(b) JPEG Compression

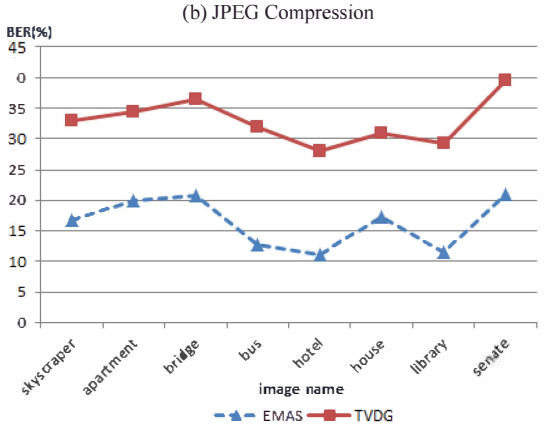

(c) Additive noise (noise intensity=1.1dB)

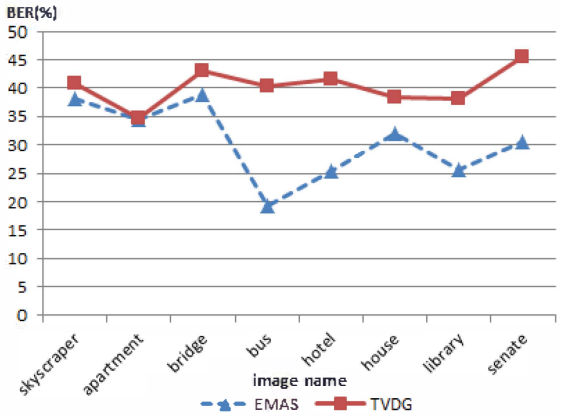

(d) JPEG Compression (quality factor=40)
Fig. 9. BER results of attacks

V. Conclusion

In this paper we propose an adaptive edge masking based on adjacent similarity for watermarking. Edge information is extracted from the original image through the TV decomposition and filtered into 3 kinds of directions (horizontal, vertical, diagonal). The JND value maps in different sub-bands reflect adjacent similar edge information. Experiments show that our algorithm would survive in additive noise, JPEG compression, cropping and rotation. Especially, it outstrips the watermarking scheme without edge masking. Also, this watermarking algorithm has good adaptability for images without abundant textures.

Acknowledgment

This research was supported by National Science and Technology Program (2014BAH10F00), Communication University of China Research Program (3132014XNG1426).

References

[1] Cox, I., Kilian, J., Leighton, T., & T.. Shamoon. Secure spread spectrum watermarking for multimedia. *IEEE Transaction on Image Processing*, 6(12), pp.1673 - 1687. 1997.

[2] Kankanhalli, M. S., R. Ramakrishnan, K., & Rajmohan. Content based watermarking of images. *Acm Multimedia*, pp.61 - 70. 1998.

[3] Barni, M., Bartolini, F., & Piva, A. Improved wavelet-based watermarking through pixel-wise masking. *IEEE Transactions on Image Processing*, 10(5), pp.783 – 791. 2001.

[4] Parthasarathy, A. K., & al., E. An improved method of content based image watermarking. *IEEE Transactions on Broadcasting*, 53(2), pp.468 - 479. 2007.

[5] Qi, X., & Qi, J. A robust content-based digital image watermarking scheme. *Signal Processing*, 87, pp.1264–1280. 2007.

[6] Wu, J., Qi, F., & Shi, G. An improved model of pixel adaptive just-noticeable difference estimation. *Acoustics Speech and Signal Processing (ICASSP), 2010 IEEE International Conference on*, 130(5), pp.2454 - 2457. 2010.

[7] Li, N., Hancock, E., Zheng, X., & Han, L. Improved content-based watermarking using scale-invariant feature points. *Lecture Notes in Computer Science*, 6978(1), pp.636-649. 2011.

[8] Wang, Y., Bai, X., & Yan, S. Digital image watermarking based on texture block and edge detection in the discrete wavelet domain. *International Conference on Sensor Network Security Technology & Privacy Communication System*, pp.170 - 174. 2013.

[9] Netravali A. N., Haskell B.G. Digital Pictures: Representation and Compression. *New York and London, Plenum Press*, 1988.

[10] Netravali A. N., Limb J. O., Picture coding: A review. *Proceedings of the IEEE*, 68(3), pp.366~406. 1980.

[11] Xu, L., Yan, Q., Xia, Y., & Jia, J. Structure extraction from texture via relative total variation. *Acm Transactions on Graphics*, 31(6), pp.439-445. 2012.

[12] Rudin, L. I., Osher, S., & Fatemi, E. Nonlinear total variation based noise removal algorithms. *Physica D Nonlinear Phenomena*, 60(1-4), pp.259–268. 1992.